Check for updates

Extraction of PEDOT:PSS/c-Si Junction Properties by Modeling of Injection-Dependent Lifetime Measurements Including Depletion Region Modulation

Marc-Uwe Halbich and Jan Schmidt**

The carrier lifetime of n-type silicon wafers coated with the conducting polymer PEDOT:PSS as a function of the excess carrier concentration Δp within the wafer is characterized using the quasi-steady-state photoconductance (QSSPC) method, and a drastic increase in the measured apparent lifetime τ_{app} with decreasing Δp is observed. The observed increase with the depletion region modulation (DRM) effect is explained, as PEDOT:PSS-coated p-type silicon wafers do not show any increase in lifetime toward low injection levels. By modeling the measured $\tau_{app}(\Delta p)$ curves on n-type silicon including interface recombination as well as the DRM effect, the interface recombination velocity as well as the band bending Ψ_s within the silicon induced by PEDOT:PSS are able to be extracted. The impact of adding sorbitol to the PEDOT:PSS dispersion on the $\tau_{app}(\Delta p)$ curves is examined, and it is demonstrated that the admixture of sorbitol improves chemical interface passivation but leaves the band bending within the silicon bulk toward the PEDOT:PSS/c-Si interface unaffected.

1. Introduction

The hole-conducting polymer poly(3,4-ethylenedioxythiophene): poly(styrene-sulfonic acid) [PEDOT:PSS] is known to effectively passivate crystalline silicon (c-Si) surfaces and simultaneously provide low contact resistance for holes.[1] PEDOT:PSS can hence be applied as a hole-selective passivating contact layer in silicon solar cells.[2–9]

Sorbitol, which has already been established as a conductance-enhancing additive to PEDOT:PSS,[10,11] can be added to reduce the parasitic absorption in PEDOT:PSS.[12] However, it turned out that sorbitol not only increases the transparency of the PEDOT:PSS layer, but also improves the passivation quality of the c-Si surface.[13] Various characterization methods have been applied to electronically analyze the PEDOT:PSS/c-Si junction,[14–16] which either require special sample preparation with contacts or advanced ultrahigh-vacuum equipment. In this study, we carry out easy-to-apply contactless injection-dependent lifetime measurements using the quasi-steady-state photoconductance (QSSPC) approach.[17,18] Our lifetime measurements are carried out on n-type silicon wafers coated with PEDOT:PSS, where we observe a very sharp increase in lifetime with decreasing injection level at very low injection densities, which we attribute to the modulation of the depletion region width at the surface of the measured silicon sample. This so-called "depletion region modulation" (DRM) effect is observed in photoconductance-based lifetime measurements if a depletion region is present at the sample's surface, e.g., due to fixed charges within a surface-passivating dielectric layer[19] or due to a p–n junction.[20] In this contribution, we demonstrate that the DRM effect can be exploited to determine the band bending in silicon and the interface passivation of organic silicon heterojunctions.

2. Experimental Section

Silicon lifetime samples were fabricated on (100)-oriented 300 μm-thick n-type Cz–Si wafers with a resistivity of 1.5 Ω cm and on p-type Fz–Si wafers with a resistivity of 1.3 Ω cm. A cross section of the fabricated lifetime samples is shown in Figure 3. One wafer surface of the n-type silicon wafers was passivated by a 100 nm-thick plasma-enhanced chemical vapor-deposited (PECVD) SiN_y layer (Plasmalab 80 Plus, Oxford Instruments) with a refractive index of $n = 2.4$ (at a wavelength of $\lambda = 633$ nm), deposited at 400 °C. As SiN_y on c-Si is known to carry a positive fixed charge density,[21] no depletion region was formed on n-type silicon. On p-type silicon, a negative charge dielectric layer has to be applied to avoid any depletion region formation. Hence, on p-type silicon wafers, we deposited a 10 nm-thick negative charge AlO_x layer by means of plasma-assisted atomic layer deposition (FlexAL, Oxford Instruments)

M.-U. Halbich, Prof. J. Schmidt
Institute for Solar Energy Research Hamelin (ISFH)
Am Ohrberg 1, Emmerthal 31860, Germany
E-mail: halbich@isfh.de; j.schmidt@isfh.de

M.-U. Halbich, Prof. J. Schmidt
Institute of Solid-State Physics
Leibniz University Hannover
Appelstr. 2, Hannover 30167, Germany

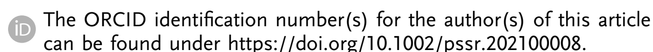
The ORCID identification number(s) for the author(s) of this article can be found under https://doi.org/10.1002/pssr.202100008.

© 2021 The Authors. Physica Status Solidi (RRL) – Rapid Research Letters published by Wiley-VCH GmbH. This is an open access article under the terms of the Creative Commons Attribution-NonCommercial-NoDerivs License, which permits use and distribution in any medium, provided the original work is properly cited, the use is non-commercial and no modifications or adaptations are made.

DOI: 10.1002/pssr.202100008

on one wafer surface,[22] which was then capped by a SiN_y layer as an etch protection layer in the subsequent etching step. To fully activate AlO_x passivation, p-type silicon wafers were thermally annealed on a hotplate at 425 °C for 15 min. All samples (n- as well as p-type) were then dipped in 1% hydrofluoric (HF) acid for 60 s to remove any native oxide from the nonpassivated wafer surface. Immediately after the HF dip, PEDOT:PSS dispersion (Clevios, Heraeus Deutschland GmbH) was deposited by spin coating (WS-650Mz-8NPPB/UD3, Laurell Technologies). PEDOT:PSS deposition was conducted by spin coating at a rotational speed of 500 rpm for 10 s and 1500 rpm for 30 s. Subsequently, the PEDOT:PSS layer was annealed on a hotplate for 10 min at 130 °C in ambient environment. Note that we used samples coated only on one side with PEDOT:PSS, as samples coated on both sides with PEDOT:PSS showed a degradation of the passivation quality due to the additional annealing step at 130 °C. Injection-dependent measurements of the carrier lifetime were carried out at 30 °C by a Sinton Lifetime Tester (WCT-120, Sinton Instruments) using the QSSPC method.

2.1. Interface Model

Measurements of the photoconductance versus the illumination intensity can be used to determine the effective recombination lifetime τ_{eff} of Si wafers. It is well known that minority-carrier trapping may cause the measured apparent effective excess carrier lifetime τ_{app} to be larger than the actual recombination lifetime τ_{eff}.[23,24] However, a drastic overestimation of the measured lifetime cannot only be caused by minority-carrier trapping centers in the silicon bulk, but also by the presence of a junction leading to a depletion region at the sample's surface. Excess charge carriers may accumulate at the edge of the depletion region, reducing the width of the depletion region. The width of the depletion region decreases with increasing light intensity. This effect named DRM in the literature[19,20] was reported on c-Si samples with dopant-diffused p–n junctions and c-Si wafers passivated with charged dielectric layers.[19]

Under illumination, the presence of a depletion region within an n-type silicon sample leads to the appearance of additional excess carrier densities Δp_{DRM} in the sample in addition to the bulk excess carrier concentration Δp. As c-Si surfaces coated with PEDOT:PSS are due to band bending known to lead to an increase of holes close to n-type silicon surfaces,[25] one would expect to observe a DRM effect also in PEDOT:PSS n-type silicon samples. A band diagram of the physical situation of band bending at the surface of an n-type silicon wafer with a negative surface charge Q_f is schematically shown in Figure 5. This situation is equivalent to the PEDOT:PSS/n-Si interface but easier to model. If Δp and Δp_{DRM} are of the same order of magnitude, which may be the case in low injection levels, the additional charge carriers Δp_{DRM} lead to an overestimation in the measured carrier lifetime.[19,20] The measured photoconductance is equal to the conductance of silicon under illumination σ_{light} minus the conductance without excess charge carriers σ_{dark}, i.e., without illumination.

$$\Delta p = \frac{\sigma_{light} - \sigma_{dark}}{qW(\mu_n + \mu_p)} \tag{1}$$

The conductance is composed of the fraction of the conductance without band bending σ_{fb} plus the conductance induced by band bending σ_{bb}[19]

$$\sigma = \sigma_{fb} + \sigma_{bb} \tag{2}$$

where σ_{fb} is given by

$$\sigma_{fb} = qW[(n_0 + \Delta p)\mu_n + (p_0 + \Delta p)\mu_p] \tag{3}$$

σ_{bb} describes the deviation of the conductance due to band bending Ψ_s at the silicon surface and is described by solving the Poisson equation near the silicon surface.[19–20,26]

$$\sigma_{bb}(\Psi_s) = \pm\sqrt{\frac{q^2\varepsilon_0\varepsilon_{Si}}{2k_BT}} \int_0^{\Psi_s} \frac{(n_0 + \Delta p)(\exp(\frac{q\Psi}{k_BT}) - 1)\mu_n + (p_0 + \Delta p)(\exp(\frac{-q\Psi}{k_BT}) - 1)\mu_p}{\sqrt{F(\Psi, \Delta p)}} d\Psi \tag{4}$$

where $\sqrt{F(\Psi, \Delta p)}$ is the auxiliary function given by

$$\sqrt{F(\Psi, \Delta p)} = (n_0 + \Delta p)\left(\exp\left(\frac{q\Psi}{k_BT}\right) - 1\right) + (p_0 + \Delta p)\left(\exp\left(\frac{-q\Psi}{k_BT}\right) - 1\right) + \frac{q\Psi(N_A - N_D)}{k_BT} \tag{5}$$

With the value for Ψ_s determined according to Girisch et al.,[27] the conductance σ_{bb} can be calculated as a function of the band bending Ψ_s at the silicon surface and the excess carrier concentration p in the bulk. The overall excess carrier concentration Δp_{total}, which includes the excess charge carriers due to the band bending at the silicon surface, can be calculated using the equation

$$\Delta p_{total} = \Delta p_{fb} + \Delta p_{bb} \tag{6}$$

where Δp_{fb} is the excess carrier concentration for flat-band conditions given by

$$\Delta p_{fb} = \frac{\sigma_{fb,light} - \sigma_{fb,dark}}{qW(\mu_n + \mu_p)} \tag{7}$$

The excess carrier concentration as a function of the band bending Δp_{bb} at the surface is given by

$$\Delta p_{bb} = \frac{\sigma_{bb,light}(\Psi_{s,light}) - \sigma_{bb,dark}(\Psi_{s,dark})}{qW(\mu_n + \mu_p)} \tag{8}$$

Finally, the apparent carrier lifetime τ_{app} is given by[26]

$$\tau_{app} = \frac{\Delta p_{total}}{G} \tag{9}$$

© 2021 The Authors. Physica Status Solidi (RRL) – Rapid Research Letters published by Wiley-VCH GmbH

where G is the corresponding photogeneration rate, which equals the total recombination rate within the sample. Note that in the case of symmetrical samples σ_{bb} and Δp_{bb} were multiplied by the factor of 2. Using Equation (6)–(9), the photoconductance-based-measured apparent lifetime τ_{app} as a function of the excess carrier concentration $\Delta p = \Delta p_{total}$ was numerically calculated for a silicon sample with induced band bending Ψ_s. With the known electron and hole densities in equilibrium n_0 and p_0, the thickness W of the silicon wafer and the quasi-Fermi levels of electrons and holes were calculated. Next, a "virtual" surface charge Q_f was assumed and the iterative procedure of Girisch et al. determined the surface potential Ψ_s.[27] The interface charge Q_{it} was neglected here, because Q_{it} is at least an order of magnitude smaller than Q_f.[28] The surface recombination velocity parameters for electrons and holes S_{n0} and S_{p0} describe the surface recombination without band bending, i.e., the level of chemical interface passivation. The recombination rate at the surface can be described by the approximative equation[29]

$$R_s = \frac{(n_s p_s - n_i^2) S_{n0} S_{p0}}{S_{n0}(n_s + n_0) + S_{p0}(p_s + p_0)} \tag{10}$$

where n_s and p_s are the carrier concentrations at the surface, which depend on the surface potential Ψ_s and the excess carrier concentrations in the bulk. Note that Equation (9) is simplified and the parameters S_{n0} and S_{p0} can be regarded as lumped parameters describing the chemical interface recombination. In reality, the interface defects are described by a quasicontinuous interface state density, whereas, in Equation (10), a discrete midgap defect level is assumed, as it is frequently done in numerical device simulations.[29] For our exemplary calculations, we identified the silicon bulk lifetime with the Auger lifetime and used the parameterization of Veith-Wolf et al.[30] **Figure 1** shows calculated apparent lifetime curves τ_{app} as a function of the excess carrier concentration Δp for different negative surface charges Q_f on the surface of an 1.5 Ω cm n-type silicon wafer for surface recombination velocities of $S_{n0} = S_{p0} = 10^2$ cm s^{-1}. Apparent lifetime curves for positive surfaces charges Q_f on n-type silicon are shown in **Figure 2**. The dashed lines are calculations without the deviation due to the band bending at the surface, i.e., without the term σ_{bb} in Equation (2). It is obvious from Figure 1 that an up-bending (as shown in Figure 5) of the energy bands toward the silicon surface (in this case due to negative fixed charges on top) leads to a drastic apparent increase in lifetime with decreasing Δp. With increasing band bending, the DRM effect shifts to larger injection densities. However, for down-bending of energy bands (see Figure 2, positive Q_f values), no DRM effect is observable on n-type silicon.

3. Results and Discussion

Figure 3 shows measured apparent lifetimes τ_{app} curves as a function of the excess carrier concentration Δp measured by QSSPC.

The apparent lifetime τ_{app} of the p-type silicon wafer in Figure 3 (blue squares) is approximately constant over the entire investigated Δp range. In contrast, the 1.5 Ω cm n-type Si wafer shows a strong increase in the apparent lifetime τ_{app} for decreasing Δp values below ≈10^{14} cm^{-3} (red circles). We attribute this steep increase in lifetime at low injection densities to the DRM effect. PEDOT:PSS, due to its work function of

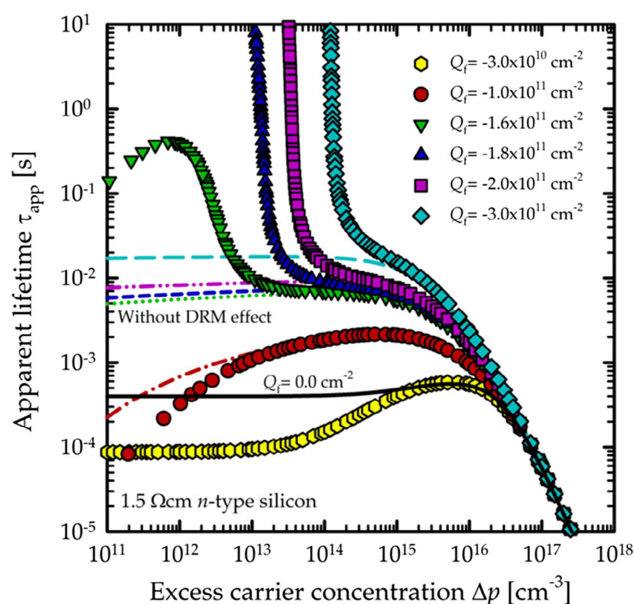

Figure 1. Theoretically calculated apparent lifetime τ_{app} as a function of the apparent excess carrier concentration Δp for different negative Q_f values and a fixed surface recombination velocity of $S_{n0} = S_{p0} = 10^2$ cm s^{-1} on a 1.5 Ω cm 300 μm-thick n-type silicon wafer. The dashed lines show the corresponding curves without the DRM effect. The black solid line corresponds to flat-band conditions.

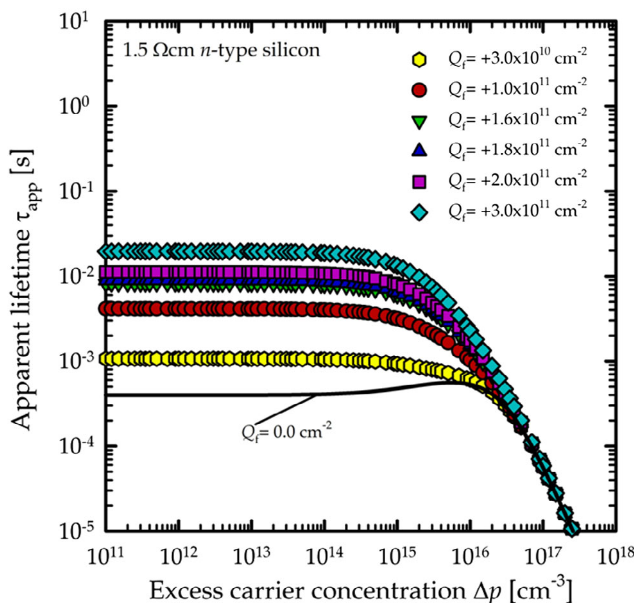

Figure 2. Theoretically calculated apparent lifetime τ_{app} as a function of the apparent excess carrier concentration Δp for different positive Q_f values and a fixed surface recombination velocity of $S_{n0} = S_{p0} = 10^2$ cm s^{-1} on a 1.5 Ω cm 300 μm-thick n-type silicon wafer. The black solid line corresponds to flat-band conditions.

© 2021 The Authors. Physica Status Solidi (RRL) – Rapid Research Letters published by Wiley-VCH GmbH

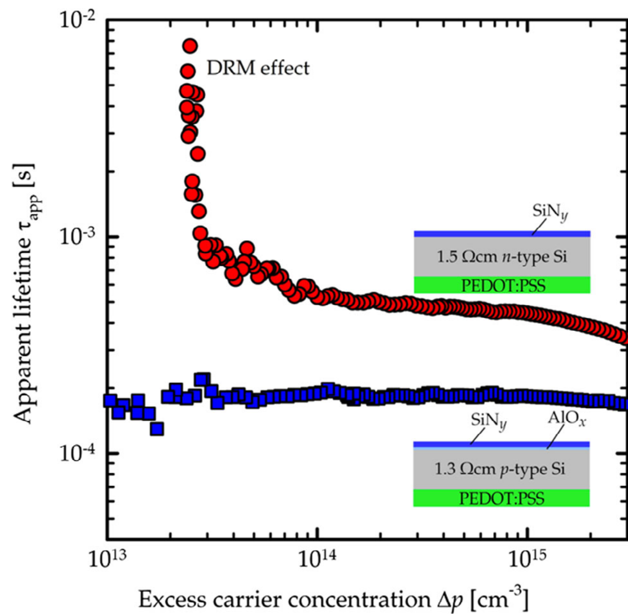

Figure 3. QSSPC-measured injection-dependent apparent lifetimes $\tau_{app}(\Delta p)$ of PEDOT:PSS-coated 1.5 Ω cm n-type silicon (red circles, opposite surface passivated with positive charge SiN_y) and 1.3 Ω cm p-type silicon (blue squares, other surface passivated with a negative charge AlO_x/SiN_y stack).

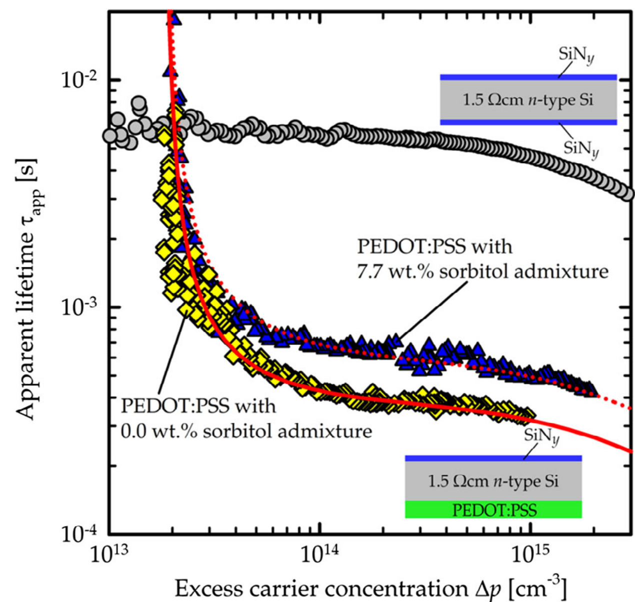

Figure 4. Experimental (symbols) and fitted (lines) apparent lifetime $\tau_{app}(\Delta p)$ curves of 1.5 Ω cm n-type Si wafers passivated with PEDOT:PSS and SiN_y. The resulting interface parameters are shown in Table 1. As a reference, the gray circles show a measurement of a both-sides SiN_y-passivated wafer with no DRM effect being visible.

5.2 eV, induces a band bending in n-type silicon, which causes an accumulation of minority carriers (i.e., holes) at the surface and thus creates a depletion region at the PEDOT:PSS/n-Si junction.[31] To model the observed lifetime increase at low injection densities, we treat the PEDOT:PSS layer in the same way as a passivating dielectric layer with a fixed negative charge density, resulting in the same kind of depletion region at the silicon surface. In our model, we not only include the change in photoconductance during quasi-steady-state measurements, but also the change in the additional conductance caused by the DRM at the PEDOT:PSS/n-Si junction. By fitting the measured apparent lifetime curves $\tau_{app}(\Delta p)$ with the simulated apparent lifetimes, we are able to determine the band bending Ψ_s induced by PEDOT:PSS at the interface in n-type silicon. **Figure 4** shows measured lifetimes of n-type silicon wafers with PEDOT:PSS/n-Si junction as a function of Δp. We also measured the apparent lifetime τ_{app} of a reference silicon wafer passivated on both sides with SiN_y (shown in Figure 4 as gray circles).

The apparent lifetime in Figure 4 of the n-type silicon wafer passivated on both sides with SiN_y (gray circles) shows no DRM effect. The apparent lifetime curves for n-type silicon wafers with PEDOT:PSS/n-Si junction clearly show the DRM effect for Δp values below $\approx 10^{14}\,\text{cm}^{-3}$. We examine here a PEDOT:PSS dispersion without and with 7.7 wt% sorbitol addition. The addition of 7.7 wt% sorbitol to the PEDOT:PSS precursor dispersion leads to a higher apparent lifetime for Δp values larger than $\approx 4 \times 10^{13}\,\text{cm}^{-3}$ (blue triangles). In previous studies we showed that the addition of sorbitol to the PEDOT:PSS precursor dispersion has a positive impact on the passivation quality of p-type silicon surfaces with PEDOT:PSS.[13,32] The fact that the addition of sorbitol improves the passivation quality of PEDOT:PSS is confirmed here on n-type silicon. For excess carrier densities below $\approx 4 \times 10^{13}\,\text{cm}^{-3}$, however, there is no difference in the DRM-affected $\tau_{app}(\Delta p)$ lifetime curves with and without sorbitol addition (compare yellow diamonds and blue triangles). With a simulation of the $\tau_{app}(\Delta p)$ dependence and a fit of our experimental data shown in Figure 4 (red lines), we can now determine the band bending Ψ_s in the n-type silicon samples and the surface recombination velocity $S_{n0} = S_{p0}$ of the PEDOT:PSS/n-Si junction. A fit was conducted for four samples without sorbitol addition and for 7.7 wt% sorbitol addition. The average values of the band bending Ψ_s and the S_{p0} values are shown in **Table 1**. The uncertainties indicate the deviations from the mean values. Due to the sign convention, a band bending Ψ_s, which leads to an accumulation of holes, is negative.

Figure 5 shows the resulting electronic band structure for a PEDOT:PSS-coated n-type silicon wafer with doping concentration of $N_D = 3.2 \times 10^{15}\,\text{cm}^{-3}$. Our extracted value for the band bending Ψ_s, based on modeling the DRM effect, is shown in green. The Fermi energy of intrinsic silicon E_i (gray), bandgap of silicon E_g (orange), and the Fermi energy E_F (blue) are also shown.

In the literature, Jäckle et al.[25] also determined the band bending Ψ_s on PEDOT:PSS-coated n-type silicon with doping concentration of $1.5 \times 10^{15}\,\text{cm}^{-3}$. Jäckle et al.[14] reported Ψ_s values between −712 and −690 meV for PEDOT:PSS/n-Si junctions by means of capacitance–voltage (C–V) measurements. Wan et al.[15] also reported a band bending of −716 meV at the PEDOT:PSS/n-Si junction extracted from C–V measurements. Wang et al.[16] reported a band bending for the PEDOT:PSS/n-Si junction of −710 meV, as determined by X-ray photoelectron spectroscopy (XPS) and ultraviolet photoelectron spectroscopy (UPS). Within the range of the measurement

© 2021 The Authors. Physica Status Solidi (RRL) – Rapid Research Letters published by Wiley-VCH GmbH

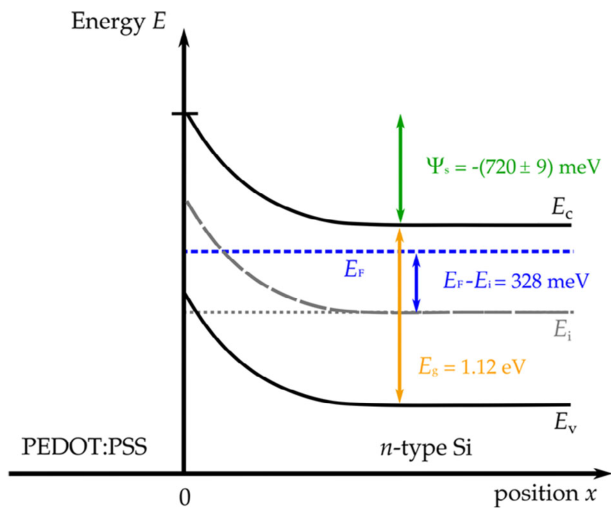

Figure 5. Schematic of the electronic band structure in a PEDOT:PSS-coated n-type silicon wafer with doping concentration of $N_D = 3.2 \times 10^{15}\,cm^{-3}$. Our extracted value for the band bending Ψ_s, based on fitting the DRM effect to injection-dependent lifetime measurements, is shown in green.

Table 1. Interface parameters Ψ_s and $S_{n0} = S_{p0}$, determined by fitting the experimental data shown in Figure 4.

Sorbitol content of PEDOT:PSS dispersion c_{sorb} [wt%]	Band bending in 1.5 Ω cm n-type silicon Ψ_s [meV]	Surface recombination velocity parameter $S_{p0} = S_{n0}$ [cm s^{-1}]
0.0 (4 samples)	$-(720 \pm 9)$	$(2.2 \pm 0.2) \times 10^3$
7.7 (4 samples)	$-(714 \pm 6)$	$(1.5 \pm 0.1) \times 10^3$

uncertainties, the band bending Ψ_s determined by the contactless easy-to-apply method introduced in this article is in excellent agreement with the Ψ_s values reported in the literature based on advanced characterization techniques. Interestingly, within the measurement uncertainty, we do not observe any impact of sorbitol admixture to PEDOT:PSS on Ψ_s. However, the addition of sorbitol improves the chemical interface passivation by ≈30%.

4. Conclusion

We have shown that lifetime curves obtained from QSSPC measurements on n-type silicon wafers coated with PEDOT:PSS show a drastic increase in the measured apparent lifetime with decreasing injection density Δp. We have attributed this increase to the DRM effect. As expected, injection-dependent lifetime curves of PEDOT:PSS-coated p-type silicon wafers did not show any DRM effect. We have modeled the $\tau_{app}(\Delta p)$ curves including the DRM effect at the PEDOT:PSS/n-Si junction. By modeling the measured $\tau_{app}(\Delta p)$ curves, we were able to extract the PEDOT:PSS-induced band bending Ψ_s in silicon toward the interface. The determined value for the band bending Ψ_s of $-(720 \pm 9)$ meV is in good agreement with values reported in the literature for the PEDOT:PSS/c-Si junction obtained from capacitance–voltage (C–V), XPS, and UPS measurements. The introduced contactless method to determine Ψ_s from injection-dependent lifetime measurements was hence demonstrated to be well suitable to analyze the electronic properties of organic silicon heterojunctions. We also examined the impact of adding sorbitol to PEDOT:PSS dispersion on the DRM effect. Within the measurement uncertainty range, we did not observe any impact of the sorbitol admixture on the band bending Ψ_s. The interface recombination, however, decreased significantly by the admixture of sorbitol. Hence, we conclude that the admixture of sorbitol to PEDOT:PSS improves the chemical interface passivation of the PEDOT:PSS/c-Si junction but leaves the band bending within the silicon unchanged.

Acknowledgements

This work was funded by the German State of Lower Saxony. The content is the responsibility of the authors.

Open access funding enabled and organized by Projekt DEAL.

Conflict of Interest

The authors declare no conflict of interest.

Data Availability Statement

The data that support the findings of this study are available from the corresponding author upon reasonable request.

Keywords

carrier lifetimes, depletion region modulation, heterojunctions, PEDOT:PSS, silicon

Received: January 6, 2021
Revised: January 22, 2021
Published online: February 11, 2021

[1] J. Schmidt, V. Titova, D. Zielke, *Appl. Phys. Lett.* **2013**, *103*, 183901.
[2] L. He, C. Jiang, H. Wang, D. Lai, Rusli, *Appl. Phys. Lett.* **2012**, *100*, 073503.
[3] R. Gogolin, D. Zielke, A. Descoeudres, M. Despeisse, C. Ballif, J. Schmidt, *Energy Procedia* **2017**, *124*, 593.
[4] D. Zielke, A. Pazidis, F. Werner, J. Schmidt, *Sol. Energy Mater. Sol. Cells* **2014**, *131*, 110.
[5] D. Zielke, C. Niehaves, W. Lövenich, A. Elschner, M. Hörteis, J. Schmidt, *Energy Procedia* **2015**, *77*, 331.
[6] Y. Zhang, R. Liu, S. T. Lee, B. Sun, *Appl. Phys. Lett.* **2015**, *104*, 083514.
[7] M. Pietsch, S. Jäckle, S. H. Christiansen, *Appl. Phys. A* **2014**, *115*, 1109.
[8] H. Wen, H. Cai, Y. Du, X. Dai, Y. Sun, J. Ni, J. Li, D. Zhang, J. Zhang, *Appl. Phys. A* **2017**, *123*, 14.
[9] Y. Liu, Y. Li, Y. Wu, G. Yang, L. Mazzarella, P. Procel-Moya, A. C. Tamboli, K. Weber, M. Boccard, O. Isabella, X. Yang, B. Sun, *Mater. Sci. Eng. R* **2020**, *142*, 100579.
[10] F. Jonas, A. Karbach, B. Muys, E. van Thillo, R. Wehrmann, A. Elschner, R. Dujardin, (Bayer AG), *Ger. EP 0 686 662 B1*, **1995**.
[11] S. Timpanaro, M. Kemerink, F. J. Touwslager, M. M. De Kok, S. Schrader, *Chem. Phys. Lett.* **2004**, *394*, 339.

© 2021 The Authors. Physica Status Solidi (RRL) – Rapid Research Letters published by Wiley-VCH GmbH

[12] M.-U. Halbich, D. Zielke, R. Gogolin, R. Sauer, W. Lövenich, J. Schmidt, *AIP Conf. Proc.* **2018**, *1999*, 040008.
[13] M.-U. Halbich, D. Zielke, R. Gogolin, R. Sauer-Stieglitz, W. Lövenich, J. Schmidt, *Sci. Rep.* **2019**, *9*, 9775.
[14] S. Jäckle, M. Liebhaber, C. Gersmann, M. Mews, K. Jäger, S. Christiansen, K. Lips, *Sci. Rep.* **2017**, *7*, 2170.
[15] L. Wan, C. Zhang, K. Ge, X. Yang, F. Li, W. Yan, Z. Xu, L. Yang, Y. Xu, D. Song, J. Chen, *Adv. Energy Mater.* **2020**, *10*, 1903851.
[16] R. Wang, Y. Wang, C. Wu, T. Zhai, J. Yang, B. Sun, S. Duhm, N. Koch, *Adv. Funct. Mater.* **2020**, *30*, 1903440.
[17] R. A. Sinton, *Appl. Phys. Lett.* **1996**, *69*, 2510.
[18] A. Cuevas, in *Proc. of the 2nd World Conf. on Photovoltaic Energy Conversion*, Joint Research Centre (European Commission), Vienna, Austria **1998**.
[19] M. Bail, M. Schulz, R. Brendel, *Appl. Phys. Lett.* **2003**, *82*, 757.
[20] P. J. Cousins, D. H. Neuhaus, J. E. Cotter, *J. Appl. Phys.* **2004**, *95*, 1854.
[21] R. Hezel, *Solid-State Electron.* **1981**, *24*, 863.
[22] F. Werner, Y. Larionova, D. Zielke, T. Ohrdes, J. Schmidt, *J. Appl. Phys.* **2014**, *115*, 073702.
[23] D. Macdonald, A. Cuevas, *Appl. Phys. Lett.* **1999**, *74*, 1710.
[24] D. H. Neuhaus, P. J. Cousins, A. G. Aberle, in *3rd World Conf. on Photovoltaic Energy Conversion*, IEEE, Osaka, Japan **2003**, Vol. 1, pp. 91–94.
[25] S. Jäckle, M. Mattiza, M. Liebhaber, G. Brönstrup, M. Romme, K. Lips, S. Christiansen, *Sci. Rep.* **2015**, *5*, 13008.
[26] M. Garin, I. Martin, S. Bermejo, R. Alcubilla, *J. Appl. Phys.* **2007**, *101*, 123716.
[27] R. Girisch, R. P. Mertens, R. F. de Keersmaecker, *IEEE Trans. Electron Devices* **1988**, *35*, 203.
[28] A. G. Aberle, S. Glunz, W. Warta, *J. Appl. Phys.* **1992**, *71*, 4422.
[29] P. P. Altermatt, *J. Comput. Electron.* **2011**, *10*, 314.
[30] B. A. Veith-Wolf, S. Schäfer, R. Brendel, J. Schmidt, *Sol. Energy Mater. Sol. Cells* **2018**, *186*, 194.
[31] J. Huang, P. F. Miller, J. C. de Mello, A. J. de Mello, D. D. C. Bradley, *Synth. Met.* **2003**, *139*, 569.
[32] M.-U. Halbich, R. Sauer-Stieglitz, W. Lövenich, J. Schmidt, in *Proc. 36th European Photovoltaic Energy Conf.*, WIP GmbH & Co Planungs-KG, Munich, Germany **2019**, pp. 214–218.

© 2021 The Authors. Physica Status Solidi (RRL) – Rapid Research Letters published by Wiley-VCH GmbH